Biased allosteric modulation at the CaSR engendered by structurally diverse calcimimetics

Anna E. Cook[1], Shailesh N. Mistry[2], Karen J. Gregory[1], Sebastian G.B. Furness[1], Patrick M. Sexton[1], Peter J. Scammells[2], Arthur D. Conigrave[3], Arthur Christopoulos[1] and Katie Leach[1]

[1] Drug Discovery Biology and Department of Pharmacology, Monash Institute of Pharmaceutical Sciences, Monash University, 381 Royal Parade, Parkville, 3052, VIC, Australia. [2] Medicinal Chemistry, Monash Institute of Pharmaceutical Sciences, Monash University, 381 Royal Parade, Parkville, 3052, VIC, Australia. [3] School of Molecular Bioscience, University of Sydney, 2006, NSW, Australia.

Appendix S1: Supplemental Methods

Abbreviations

calcd, calculated; DCM, dichloromethane; Et_2O, diethyl ether; EtOAc, ethyl acetate; EtOH, ethanol (absolute); FCC, flash column chromatography; MeCN, acetonitrile; PE, petroleum spirits 40-60; PLC, preparative layer chromatography; RP-HPLC, reverse phase high performance liquid chromatography; rt, room temperature; TFA, trifluoroacetic acid; THF, tetrahydrofuran; TLC, thin-layer chromatography.

Synthesis of calcimimetic compounds

Synthesis of *R,R*-calcimimetic B **(3b)**, diastereoisomer *S,R*-calcimimetic B **(3a)** and nor-calcimimetic B **(3c)** was achieved using a two-step procedure (Scheme 1), derived from described literature. (Bringmann and Geisler, 1989; Harrington et al., 2010) Initially, biphenyl intermediates **(2a)** and **(2b)** were obtained from 3-iodo-4-methoxyacetophenone **(1a)** or 3-iodo-4-methoxybenzaldehyde **(1b)** respectively, via Suzuki coupling with 4-(trifluoromethyl)phenyl boronic acid. Subsequent reductive amination in the presence of $TiCl_4$, using $NaBH_4$ afforded the desired compounds **(3a-c)**. *R,R*-Calcimimetic B **(3b)** and

diastereoisomer *S,R*-Calcimimetic B **(3a)** were isolated by separation of reaction mixture crude products by either chiral chromatography or PLC.

Scheme 1: Synthesis of analogues of Calcimimetic compounds[a]

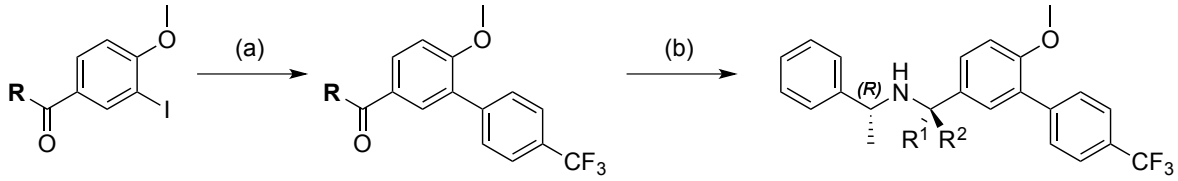

1a **R =** Me
1b **R =** H

2a **R =** Me
2b **R =** H

3a **R^1 =** Me; **R^2** = H (*S,R*-calcimimetic B)
3b **R^1 =** H; **R^2** = Me (*R,R*-calcimimetic B)
3c **R^1 = R^2** = H (nor-calcimimetic B)

[a] Reagents and conditions: (a) 4-(trifluoromethyl)phenyl boronic acid, 1M Na_2CO_3, $PdCl_2(PPh_3)_2$, THF, 100 °C, 72-75%; (b) i. (*R*)-(+)-α-methylbenzylamine, $TiCl_4$, DCM, 0 °C to rt; ii. $NaBH_4$, EtOH, rt, 31-81%;

General Chemistry Methods: Chemicals and solvents were purchased from standard suppliers and used without further purification. Davisil® silica gel (40-63μm), for flash column chromatography was supplied by Grace Davison Discovery Sciences (Victoria, Australia) and deuterated solvents were purchased from Cambridge Isotope Laboratories, Inc. (USA, distributed by Novachem Pty. Ltd, Victoria, Australia).

Unless otherwise stated, reactions were carried out at ambient temperature. All microwave reactions took place in a Biotage Initiator Microwave Synthesiser. Reactions were monitored by thin layer chromatography on commercially available precoated aluminium-backed plates (Merck Kieselgel 60 F_{254}). Visualisation was by examination under UV light (254 and 366 nm). General staining carried out with $KMnO_4$ or phosphomolybdic acid. A solution of Ninhydrin (in ethanol) was used to visualize primary and secondary amines. All organic extracts collected after aqueous work-up procedures were dried over anhydrous $MgSO_4$ or Na_2SO_4 before gravity filtering and evaporation to dryness. Organic solvents were evaporated *in vacuo* at ≤ 40°C (water bath temperature). Purification using preparative layer

chromatography (PLC) was carried out on Analtech preparative TLC plates (200 mm x 200 mm x 2 mm).

High-resolution mass spectra (HRMS) were obtained from a Waters LCT Premier XE (TOF) mass spectrometer fitted with an ESI ion source, coupled to a 2795 Alliance Separations Module. ^{1}H NMR and ^{13}C NMR spectra were recorded on a Bruker Avance Nanobay III 400MHz Ultrashield Plus spectrometer at 400.13 MHz and 100.62 MHz respectively. Chemical shifts (δ) are recorded in parts per million (ppm) with reference to the chemical shift of the deuterated solvent. Coupling constants (*J*) and carbon-fluorine coupling constants (J_{CF}) are recorded in Hz and the significant multiplicities described by singlet (s), doublet (d), triplet (t), quadruplet (q), broad (br), multiplet (m), doublet of doublets (dd), doublet of triplets (dt). Spectra were assigned using appropriate COSY, distortionless enhanced polarisation transfer (DEPT), HSQC and HMBC sequences.

LCMS were run to verify reaction outcome and purity using an Agilent 6100 Series Single Quad coupled to an Agilent 1200 Series HPLC. The following buffers were used; buffer A: 0.1% formic acid in H_2O; buffer B: 0.1% formic acid in MeCN. The following gradient was used with a Phenomenex Luna 3μM C8(2) 15 x 4.6 mm column, and a flow rate of 0.5 mL/min and total run time of 12 min; 0–4 min 95% buffer A and 5% buffer B, 4–7 min 0% buffer A and 100% buffer B, 7–12 min 95% buffer A and 5% buffer B. Mass spectra were acquired in positive and negative ion mode with a scan range of 0–1000 *m/z* at 5V. UV detection was carried out at 254 nm. All retention times (t_R) are quoted in minutes. All compounds were of > 95% purity.

1-(6-Methoxy-4'-(trifluoromethyl)-[1,1'-biphenyl]-3-yl)ethanone (2a). THF (6 mL) and 1M $Na_2CO_{3\,(aq)}$ (2 mL) were mixed in a 10 mL microwave vessel and degassed by bubbling with N_2, then sonicating for 5 minutes. 3-Iodo-4-methoxyacetophenone **(1a)** (2.00 g, 7.24 mmol), 4-(trifluoromethyl)phenyl boronic acid (2.06 g, 10.87 mmol, 1.5 eq) and $PdCl_2(PPh_3)_2$

(505 mg, 0.72 mmol, 0.1 eq) were added, forming a pale orange suspension. The tube was sealed and heated at 100 °C for 2 hours. LCMS analysis indicated only product and excess boronic acid remained after this time. The mixture was diluted with EtOAc (50 mL) and filtered through a bed of Celite. The filtrate was then washed with water (2 x 30 mL), and brine (30 mL), before drying over $MgSO_4$. After concentration under reduced pressure, the crude was further purified by FCC (eluent EtOAc/PE 0:100 to 20:80) to give 1.404 g of pale brown oil, which slowly crystallised. Although TLC analysis (EtOAc/PE 3:7) showed only one spot, LCMS indicated there was still some 3-iodo-4-methoxyacetophenone **(1a)** present. Further analysis by 1H-NMR indicated around 55% conversion had taken place. The reaction was restarted using the same volume of solvent and base, adding 4-(trifluromethyl)phenyl boronic acid (1.37 g, 1 eq) and $PdCl_2(PPh_3)_2$ and heating at 100 °C for a further 4.5 hours. LCMS analysis indicated complete disappearance of the starting material peak. The mixture was cooled before diluting with Et_2O (30 mL) and water (20 mL) and discarding the aqueous layer after agitation. The remaining organic layer was passed through a bed of celite, before concentration of the filtrate and further purification by FCC (EtOAc/PE 10:90), to give 1.54 g (72%) of brown oil. ^{1}H NMR (400 MHz, $CDCl_3$) δ 8.01 (dd, J = 8.6/2.3 Hz, 1H), 7.94 (d, J = 2.3 Hz, 1H), 7.72 – 7.57 (m, 4H), 7.04 (d, J = 8.7 Hz, 1H), 3.90 (s, 3H), 2.59 (s, 3H); ^{13}C NMR (101 MHz, $CDCl_3$) δ 196.74, 160.39, 141.33, 131.43, 130.66, 130.61, 129.99, 129.60 (q, J_{CF} = 33.0 Hz), 129.44, 125.18 (q, J_{CF} = 3.8 Hz), 124.39 (q, J_{CF} = 272.0 Hz), 110.87, 56.03, 26.52; *m/z* MS (TOF ES$^+$) $C_{16}H_{14}F_3O_2$ $[MH]^+$ calcd 295.1; found 295.1; RP-HPLC t_R: 6.35.

(*S*)-1-(6-methoxy-4'-(trifluoromethyl)-[1,1'-biphenyl]-3-yl)-*N*-((*R*)-1-phenylethyl)ethan-1-amine (*S,R*-calcimimetic B, 3a) and (*R*)-1-(6-Methoxy-4'-(trifluoromethyl)-[1,1'-biphenyl]-3-yl)-*N*-((*R*)-1-phenylethyl)ethan-1-amine (*R,R*-calcimimetic B, 3b). 1-(6-Methoxy-4'-(trifluoromethyl)-[1,1'-biphenyl]-3-yl)ethanone **(2a)**

(100 mg, 0.34 mmol) and (*R*)-(+)-α-methylbenzylamine (174 mg, 1.36 mmol, 4 eq) were dissolved in dry DCM (2 mL) under an atmosphere of nitrogen and cooled over an ice bath with stirring for 5 minutes. To this was added $TiCl_4$ (0.021 mL, 0.19 mmol, 0.55 eq), and stirring continued on the ice bath for a further 30 minutes, before allowing to warm to room temperature, and stir for 4.5 hours. After this time, the DCM was removed under vacuum, and replaced with dry EtOH (2 mL), before adding $NaBH_4$ (26 mg, 0.68 mmol, 2 eq). Stirring was continued at room temperature overnight. LCMS analysis after this time indicated a single peak was present, though the mass corresponded to the deaminated product. TLC analysis (MeOH/DCM 1:99, plate run twice) indicated the starting ketone had disappeared. The mixture was partitioned between sat. $NaHCO_{3\ (aq)}$ (20 mL) and DCM (20 mL), and the entire mixture filtered through a bed of Celite. The filtrate layers were separated, and the organic layer washed with water (20 mL), before drying over $MgSO_4$ and concentrating under reduced pressure. The crude product was further purified by FCC (eluent MeOH/DCM 0:100, then 1:99, then 2:98), to give 110 mg (81%) of clear colourless oil, found to be the desired product, present as a mixture of two diastereoisomers (Ratio ~1:4 by ^{1}H NMR). ^{1}H NMR (400 MHz, $CDCl_3$) δ 7.72 – 7.55 (m, 4H, 1H*), 7.40 – 7.18 (m, 6H, 1.5H*), 7.16 (d, *J* = 2.2 Hz, 1H), 6.97 (d, *J* = 8.4 Hz, 1H), 6.93 (d, *J* = 8.4 Hz, 0.25H*), 3.83 (s, 3H), 3.80 (s, 0.75H*), 3.79 – 3.73 (m, 0.25H*), 3.59 – 3.45 (m, 2H, 0.25H*), 1.55 (s, 2H, 0.5H*), 1.36 (d, *J* = 6.6 Hz, 1.5H*), 1.29 (d, *J* = 6.7 Hz, 3H), 1.28 (d, *J* = 6.7 Hz, 3H); ^{13}C NMR (101 MHz, $CDCl_3$) δ 155.43, 146.07*, 145.94, 142.52, 138.70*, 138.39, 129.98, 129.23, 129.14 (d, *J* = 2.1 Hz), 128.83*, 128.59, 128.57*, 127.71, 127.61*, 126.98, 126.74, 126.70*, 125.45, 125.01 (q, *J* = 3.8 Hz), 124.54 (q, *J* = 271.7 Hz), 111.43*, 111.39, 55.84*, 55.81, 55.27, 55.25*, 54.56, 25.24, 25.14, 23.65*, 23.38*; *Corresponds to minor diastereoisomer (some peaks overlaid); *m/z* MS (TOF ES$^+$) $C_{24}H_{24}F_3NO$ $[MH]^+$ calcd 400.2; found 279.1 (deaminated product on LCMS), 400.7 (on LRMS); RP-HPLC t_R: 5.38.

Individual diastereoisomers were separated using either PLC or chiral HPLC, as described below.

Preparative Layer Chromatography: Eluent triethylamine/*tert*-butyl methyl ether/PE (1:10:89).

Chiral HPLC: Phenomenex Lux 5μ Cellulose-2 column (150 x 4.6 mm), eluent EtOH/0.1% TFA in petroleum spirits 40-60 (1.5:98.5). This gives each diastereoisomer as the TFA salt. Subsequent desalting was achieved by PLC (eluent NH_4OH/DCM 1:99).

(*S*)-1-(6-methoxy-4'-(trifluoromethyl)-[1,1'-biphenyl]-3-yl)-*N*-((*R*)-1-phenylethyl)ethan-1-amine (*S*,*R*-calcimimetic B, 3a): 10 mg of clear colourless oil. ^{1}H NMR (400 MHz, $CDCl_3$) δ 7.71 – 7.57 (m, 4H), 7.46 – 7.16 (m, 7H), 6.93 (d, *J* = 8.5 Hz, 1H), 3.93 – 3.69 (m, 5H), 1.76 – 1.47 (m, 1H), 1.39 (s, 3H), 1.38 (s, 3H); ^{13}C NMR (101 MHz, $CDCl_3$) δ 155.57, 142.40, 142.37, 129.98, 129.66 (d, *J* = 16.8 Hz), 129.52, 129.46, 129.18, 128.62, 127.80, 127.13, 126.87, 125.00 (q, *J* = 4.0 Hz), 124.53 (d, *J* = 271.6 Hz), 111.47, 55.84, 55.39, 54.65, 20.11, 20.08; *m/z* HRMS (TOF ES$^+$) $C_{24}H_{24}F_3NO$ $[MH]^+$ calcd 400.1883; found 400.1892; $[\alpha]_D^{24}$ = - 12.38° (0.0101, DCM).

(*R*)-1-(6-Methoxy-4'-(trifluoromethyl)-[1,1'-biphenyl]-3-yl)-*N*-((*R*)-1-phenylethyl)ethan-1-amine (*R*,*R*-calcimimetic B, 3b): 66 mg of yellow oil. ^{1}H NMR (400 MHz, $CDCl_3$) δ 7.75 – 7.58 (m, 4H), 7.34 (t, *J* = 7.2 Hz, 2H), 7.30 – 7.12 (m, 5H), 6.97 (d, *J* = 8.4 Hz, 1H), 3.84 (s, 3H), 3.66 – 3.38 (m, 2H), 1.86 – 1.43 (m, 1H), 1.43 – 1.18 (m, 6H); ^{13}C NMR (101 MHz, $CDCl_3$) δ 155.51, 142.47, 142.16, 129.98, 129.54 (d, *J* = 17.3 Hz), 129.30, 129.17, 128.86, 128.62, 127.79, 127.06, 126.81, 125.01 (q, *J* = 3.8 Hz), 124.54 (d, *J* = 271.9 Hz), 111.44, 55.81, 55.37, 54.66, 25.09, 25.03; *m/z* HRMS (TOF ES$^+$) $C_{24}H_{24}F_3NO$ $[MH]^+$ calcd 400.1883; found 400.1902; $[\alpha]_D^{24}$ = + 98.50° (0.0665, DCM).

6-Methoxy-4'-(trifluoromethyl)-[1,1'-biphenyl]-3-carbaldehyde (2b). THF (3 mL) and 1M $Na_2CO_{3\ (aq)}$ (1 mL) were mixed in a 10 mL microwave vessel and degassed by bubbling

with N_2, then sonicating for 5 minutes. 3-Iodo-4-methoxybenzaldehyde **(1b)** (1.074 g, 4.10 mmol), 4-(trifluoromethyl)phenyl boronic acid (1.335 g, 12.30 mmol, 3 eq) and $PdCl_2(PPh_3)_2$ (288 mg, 0.41 mmol, 0.1 eq) were added, before sealing the vessel and heating in the microwave reactor at 100 °C for 90 mins. TLC analysis (Et_2O/PE 2:8, plate run 4 times) indicated partial progression. 1 M $Na_2CO_{3\ (aq)}$ (3.5 mL), 4-(trifluoromethyl)phenyl boronic acid (1.5 eq) and $PdCl_2(PPh_3)_2$ (0.1 eq) were added to the mixture and heating continued in the microwave reactor at 100 °C for a second 90 minutes cycle. The reaction mixture was diluted with EtOAc (30 mL) and washed with water (30 mL). The organic layer was dried over $MgSO_4$ before filtering and concentrating under reduced pressure. The crude residue was further purified by FCC (eluent EtOAc/PE 0:100 to 30:70) to give 906 mg of orange oil (75%). The compound was found to slowly oxidise to the corresponding carboxylic acid on standing at room temperature. ^{1}H NMR (400 MHz, $CDCl_3$) δ 9.95 (s, 1H), 7.92 (dd, *J* = 8.5, 2.1 Hz, 1H), 7.86 (d, *J* = 2.1 Hz, 1H), 7.69 (d, *J* = 8.3 Hz, 2H), 7.64 (d, *J* = 8.3 Hz, 2H), 7.13 (d, *J* = 8.5 Hz, 1H), 3.93 (s, 3H); ^{13}C NMR (101 MHz, $CDCl_3$) δ 190.79, 161.50, 140.92, 132.35, 132.28, 130.18, 129.96, 129.89 (d, *J* = 52.4 Hz), 129.30, 125.24 (q, *J* = 3.8 Hz), 124.36 (d, *J* = 272.1 Hz), 111.41, 56.17; *m/z* MS (TOF ES$^+$) $C_{15}H_{12}F_3O_2$ $[MH]^+$ calcd 281.1; found 281.1; RP-HPLC t_R: 6.33.

(*R*)-*N*-((6-Methoxy-4'-(trifluoromethyl)-[1,1'-biphenyl]-3-yl)methyl)-1-phenylethanamine (nor-calcimimetic B, 3c). 6-Methoxy-4'-(trifluoromethyl)-[1,1'-biphenyl]-3-carbaldehyde **(2b)** (224 mg, 0.80 mmol) underwent reductive amination with (*R*)-(+)-α-methylbenzylamine (410 mg, 3.20 mmol, 4 eq) as described above, for the synthesis of (*S*)-1-(6-methoxy-4'-(trifluoromethyl)-[1,1'-biphenyl]-3-yl)-*N*-((*R*)-1-phenylethyl)ethan-1-amine **(*S,R*-calcimimetic B, 3a)** and (*R*)-1-(6-Methoxy-4'-(trifluoromethyl)-[1,1'-biphenyl]-3-yl)-*N*-((*R*)-1-phenylethyl)ethan-1-amine **(*R,R*-calcimimetic B, 3b)**. This gave 96 mg of pale yellow oil (31%). ^{1}H NMR (400 MHz, $CDCl_3$)

δ 7.65 (d, *J* = 8.7 Hz, 2H), 7.62 (d, *J* = 8.7 Hz, 2H), 7.39 – 7.31 (m, 4H), 7.31 – 7.19 (m, 3H), 6.94 (d, *J* = 8.4 Hz, 1H), 3.91 – 3.76 (m, 4H), 3.62 (dd, *J* = 13.0 Hz, 2H), 1.74 (s, 1H), 1.38 (d, *J* = 6.6 Hz, 3H); ^{13}C NMR (101 MHz, $CDCl_3$) δ 155.57, 145.66, 142.37, 133.32, 130.82, 129.96, 129.25 (d, *J* = 3.8 Hz), 128.88, 128.65, 127.13, 126.84, 125.01 (q, *J* = 3.7 Hz), 124.44 (d, *J* = 262.1 Hz), 123.17, 111.46, 57.78, 55.86, 51.18, 24.63; *m/z* MS (TOF ES$^+$) $C_{23}H_{23}F_3NO$ $[MH]^+$ calcd 386.4; found 386.2; RP-HPLC t_R: 6.33.

Production of anti-cMyc:AF647 (9E10:AF647)

The 9E10 hybridoma (ATCC Number: CRL-1729) was maintained in a Cell-line1000 bioreactor (Integra Biosciences). The cell compartment contained DMEM supplemented with 1x HAT, 55μM 2-mercaptoethanol and 10% FBS, the medium compartment contained DMEM supplemented with 1x HAT, 55μM 2-mercaptoethanol and 3% FBS. Supernatant harvested from the cell compartment was passed through a 0.22μM filter before being buffer exchanged into PBS using 10kDa MWCO dialysis tubing over several days at 4^{o}C. Buffer exchanged hybridoma supernatant was purified over a 1mL HiTrap protein G sepharose column (GE Lifesciences) and after extensive washing was eluted using 100mM Glycine pH 2.8 and immediately neutralized with 0.05 volumes of 1M Tris pH 7.9. The purity of the eluted antibody was estimated as >90% by SDS-PAGE (supplementary figure 11A). Purified antibody was buffer exchanged into 0.1M $NaHCO_3$ pH 8.3. A 1mg lot of AF-647 carboxylic acid succinimidyl ester was made up in 100μL DMF, this was added dropwise with shaking to 10mg of antibody in 1mL of 0.1M $NaHCO_3$ pH 8.3 and reacted in the dark for 1 hour at room temperature. Unconjugated fluor and buffer exchange was achieved by repeated centrifugation in a 10kDa MWCO centrifugal concentrator (Merck Millipore). The degree of labeling of the final antibody conjugate was determined using the following equation: A_{650} x MW(150000) / ((A_{280} – (0.03 x A_{650}) x 239,000) and was 3.6. The final antibody conjugate was diluted to 10mg/mL in PBS supplemented with 25% glycerol, 0.02% sodium azide and

0.05% BSA. The antibody was validated by titration in flow cytometry using a stable Cos7 cell line transfected with either a vector control or cMyc tagged Calcitonin Receptor (Andreassen *et al.*, 2014). Briefly, cells were stained in PBS containing 5%BSA, 2mM EDTA and 0.02% sodium azide for 1 hour at 4^{o}C with 10, 5, 2.5, 1.25 and 0.625 µg/mL 9E10:AF647. Cells were washed 3x with PBS containing 0.1%BSA, 2mM EDTA and 0.02% sodium azide and finally re-suspended in this buffer with 0.5µg/mL propidium iodide for live dead discrimination. Data was analyzed using FlowJo X (Treestar) which was used to gather mean fluorescence intensity and standard deviation using >30,000 events. This data was plotted using Prism 6 (Graphpad) (Supplemental Figure 11B).

Appendix S2: Supplemental data

Supplemental Table 1. Pharmacological parameters that govern the allosteric activity of CaSR modulators in Ca^{2+}_i mobilisation, pERK1/2 and IP_1 accumulation assays. The potency of Ca^{2+}_o in the presence of increasing concentrations of modulator was fitted to an allosteric ternary complex model (Equation 2) to quantify the equilibrium dissociation constant (pK_B) and cooperativity ($\alpha\beta$) of the modulators at the human CaSR, using a model in which the binding affinity was assumed to be the same across pathways.

	pK_B ± s.e.m.	***Log$\alpha\beta$ ± s.e.m. ($\alpha\beta$)***		
		Ca^{2+}_i mobilisation	**pERK1/2**	**IP_1 accumulation**
Cinacalcet*	5.99 ± 0.14	0.66 ± 0.06 (4.6) [a]	0.45 ± 0.07 (2.8)[a]	0.72 ± 0.12 (5.2)
NPS-R568	6.47 ± 0.13	0.60 ± 0.06 (4.0)	0.58 ± 0.10 (3.8)	0.66 ± 0.10 (4.6)
Calindol	6.09 ± 0.14	0.75 ± 0.09 (5.6)	0.64 ± 0.09 (4.4)	0.70 ± 0.09 (5.0)
S,R*-Calcimimetic B	5.25 ± 0.22	0.37 ± 0.08 (2.3)	0.43 ± 0.09 (2.7)	0.78 ± 0.11 (6.0)
R,R*-Calcimimetic B	7.07 ± 0.17	0.27 ± 0.06 (1.9)	0.47 ± 0.06 (3.0)	0.49 ± 0.08 (3.1)
nor-calcimimetic B	7.05 ± 0.23	0.30 ± 0.06 (2.0)	0.32 ± 0.08 (2.1)	0.46 ± 0.09 (2.9)
AC-265347*	6.41 ± 0.13	0.63 ± 0.09 (4.3)	0.95 ± 0.08 (8.9)	0.82 ± 0.14 (6.6)

[a]Data sets taken from those used in (Leach *et al.*, 2013)

* Significant difference in *Log$\alpha\beta$* between pathways ($p<0.05$, F test)

Appendix S3: Supplemental Figures

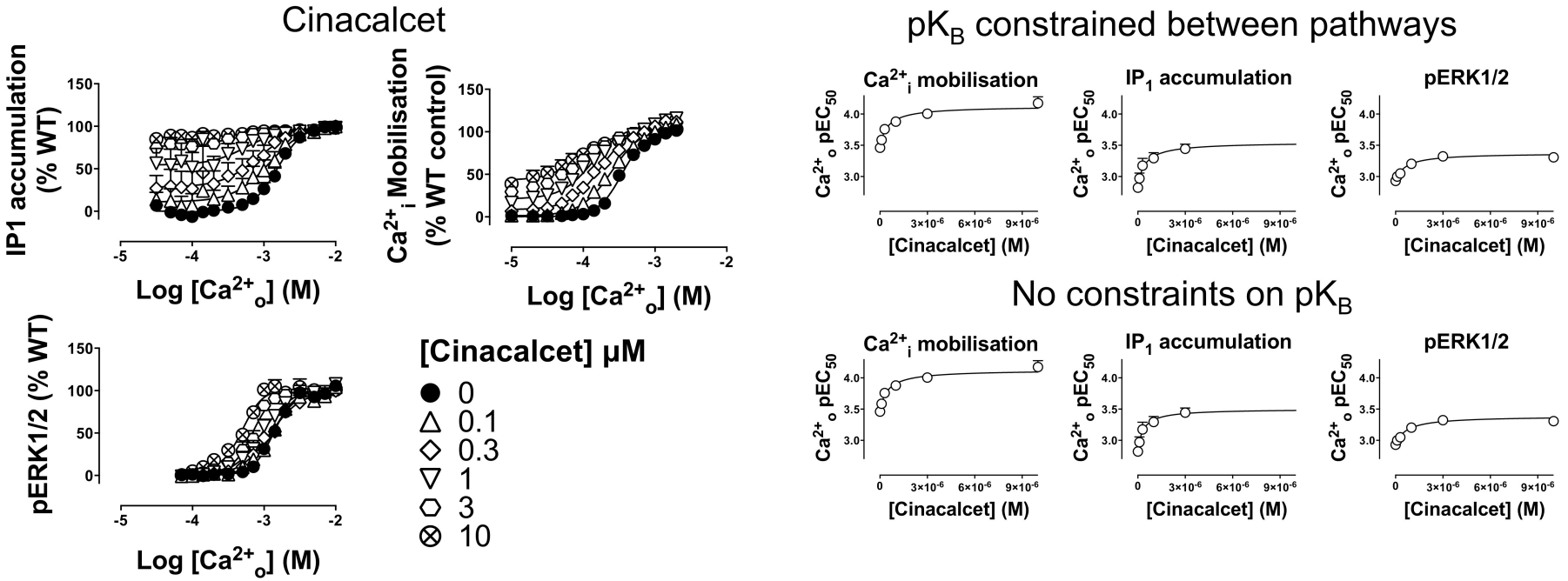

Supplemental Figure 2 Cinacalcet potentiation of Ca^{2+}_o-mediated signalling. (A) Ca^{2+}_o stimulation of IP_1 accumulation, Ca^{2+}_i mobilisation and pERK1/2 in the absence and presence of cinacalcet. (B) Non-linear regression analysis of Ca^{2+}_o potency in the absence and presence of cinacalcet with an allosteric ternary complex model (equation 2) where the pK_B is constrained between pathways or not (as indicated).

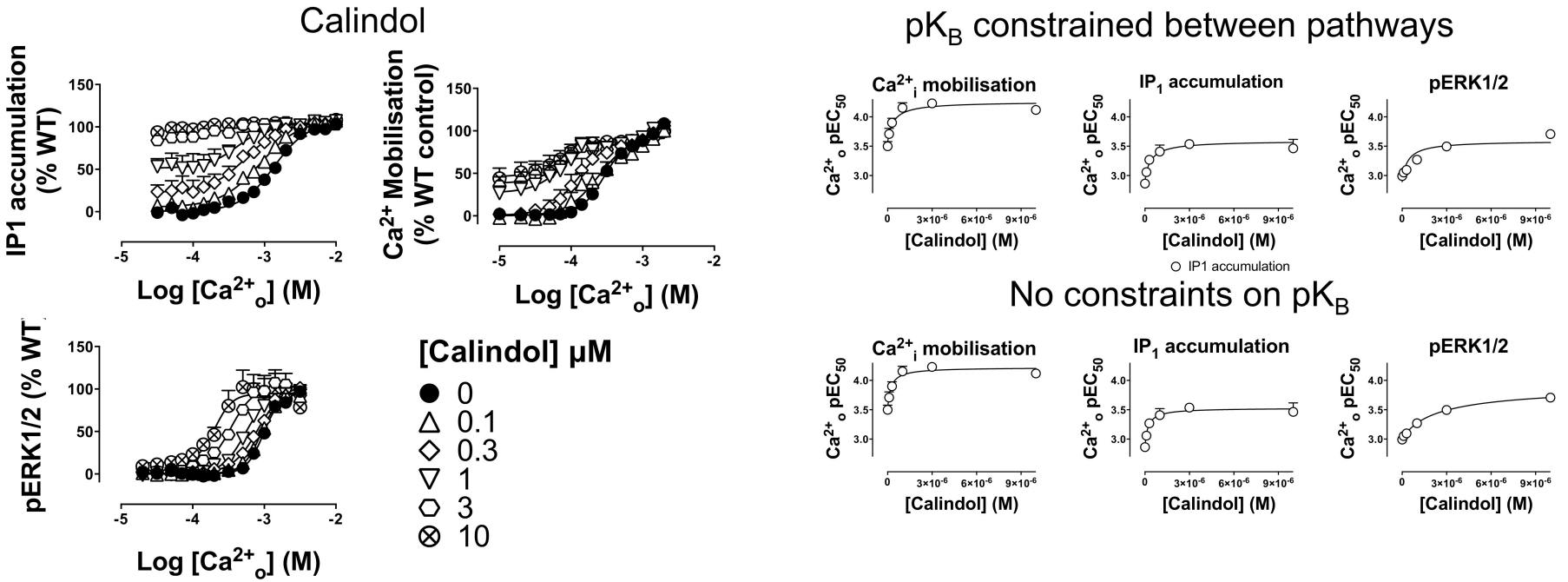

Supplemental Figure 3 Calindol potentiation of Ca^{2+}_o-mediated signalling. (A) Ca^{2+}_o stimulation of IP_1 accumulation, Ca^{2+}_i mobilisation and pERK1/2 in the absence and presence of calindol. (B) Non-linear regression analysis of Ca^{2+}_o potency in the absence and presence of calindol with an allosteric ternary complex model (equation 2) where the pK_B is constrained between pathways or not (as indicated).

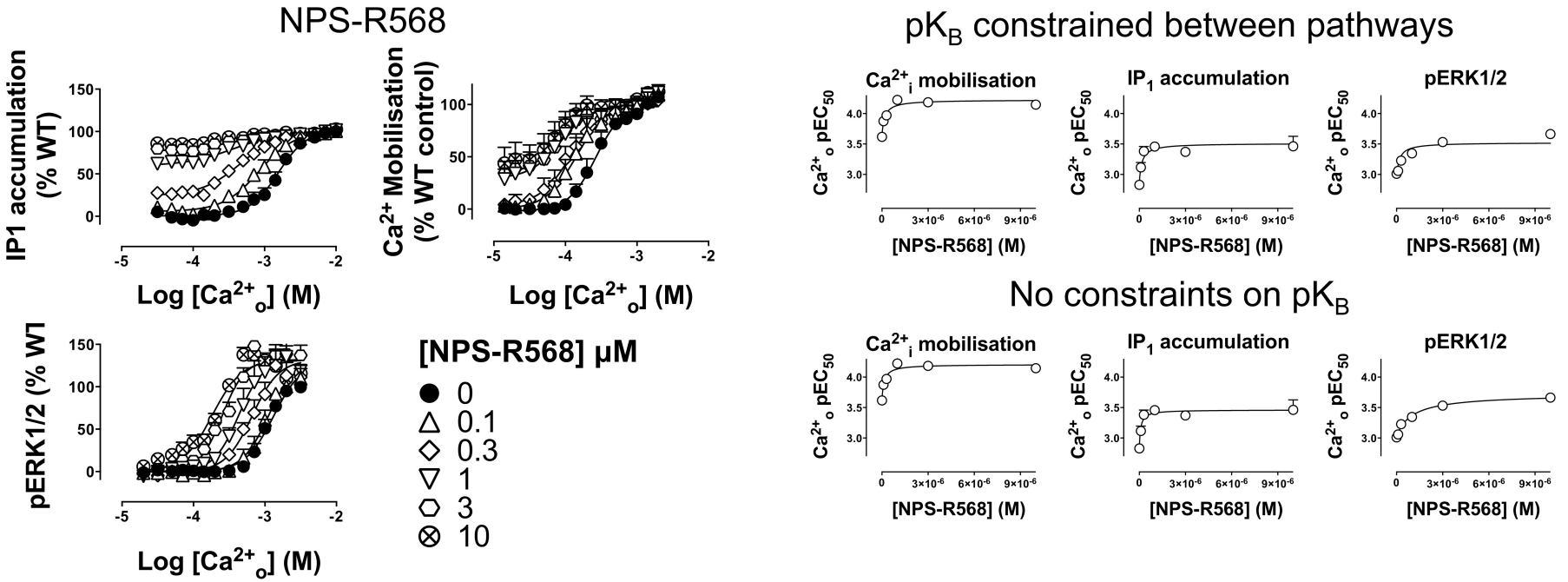

Supplemental Figure 4 NPS-R568 potentiation of Ca^{2+}_o-mediated signalling. (A) Ca^{2+}_o stimulation of IP_1 accumulation, Ca^{2+}_i mobilisation and pERK1/2 in the absence and presence of NPS-R568. (B) Non-linear regression analysis of Ca^{2+}_o potency in the absence and presence of NPR-R568 with an allosteric ternary complex model (equation 2) where the pK_B is constrained between pathways or not (as indicated).

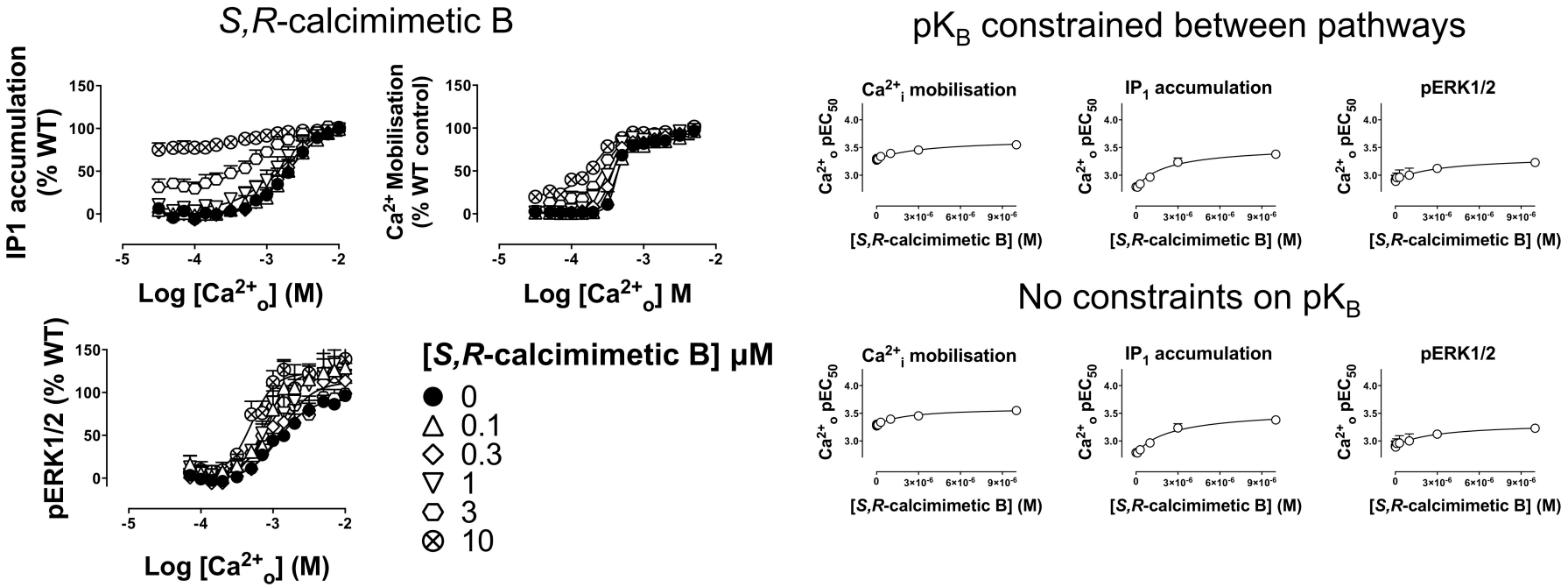

Supplemental Figure 5 *S,R*-calcimimetic B potentiation of Ca^{2+}_o-mediated signalling. (A) Ca^{2+}_o stimulation of IP_1 accumulation, Ca^{2+}_i mobilisation and pERK1/2 in the absence and presence of *S,R*-calcimimetic B. (B) Non-linear regression analysis of Ca^{2+}_o potency in the absence and presence of *S,R*-calcimimetic B with an allosteric ternary complex model (equation 2) where the pK_B is constrained between pathways or not (as indicated).

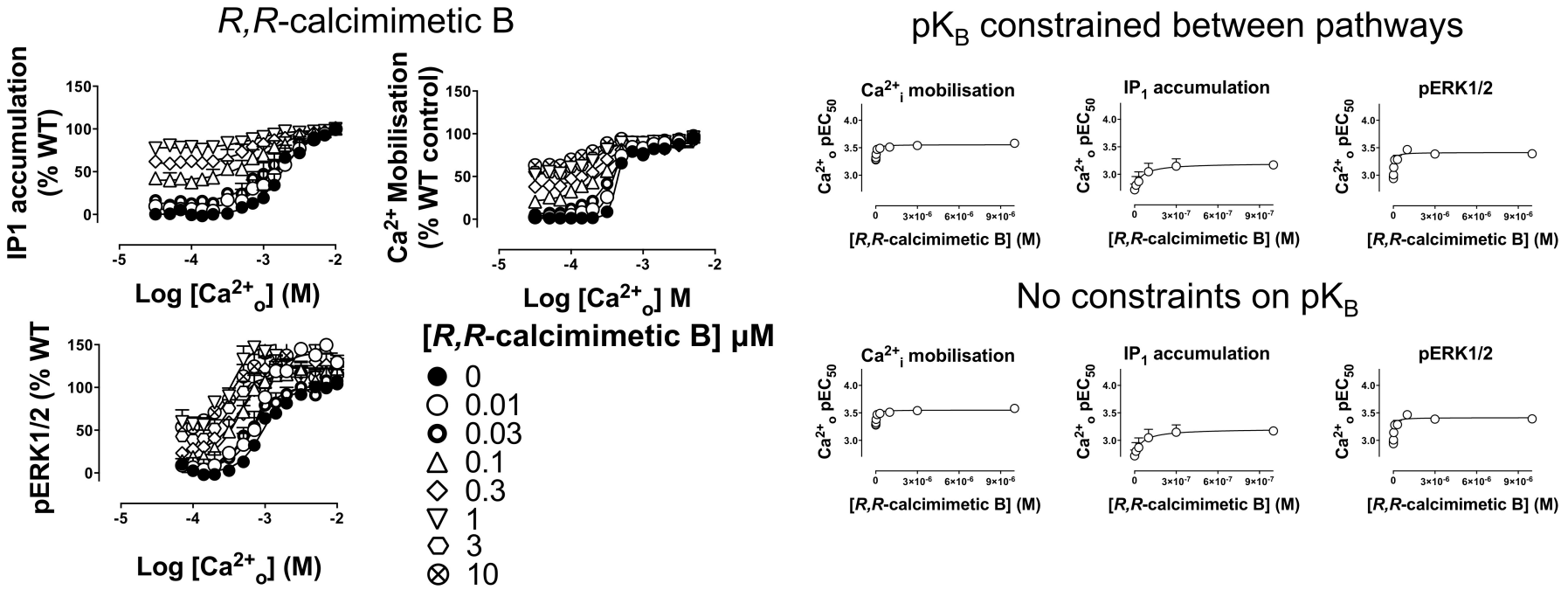

Supplemental Figure 6 *R,R*-calcimimetic B potentiation of Ca^{2+}_o-mediated signalling. (A) Ca^{2+}_o stimulation of IP_1 accumulation, Ca^{2+}_i mobilisation and pERK1/2 in the absence and presence of *R,R*-calcimimetic *B*. (B) Non-linear regression analysis of Ca^{2+}_o potency in the absence and presence of *R,R*-calcimimetic B with an allosteric ternary complex model (equation 2) where the pK_B is constrained between pathways or not (as indicated).

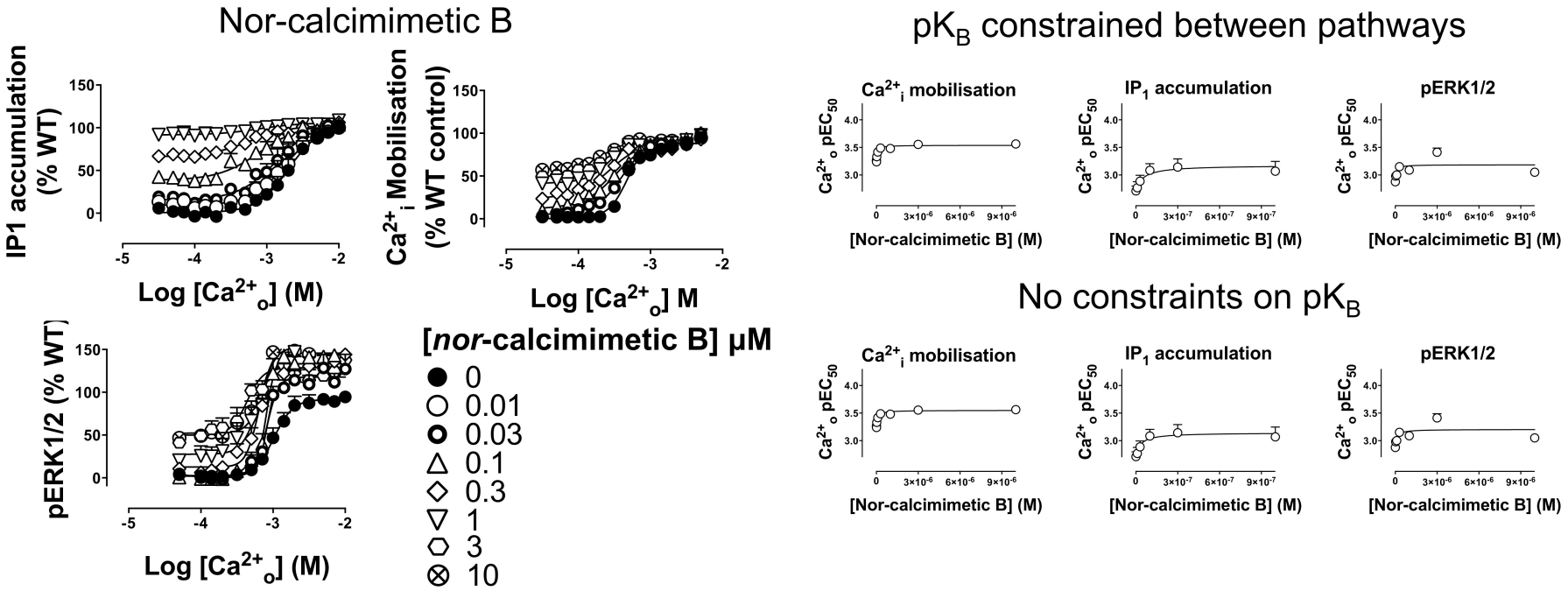

Supplemental Figure 7 ***nor*-calcimimetic B potentiation of Ca^{2+}_o-mediated signalling.** (A) Ca^{2+}_o stimulation of IP_1 accumulation, Ca^{2+}_i mobilisation and pERK1/2 in the absence and presence of *nor*-calcimimetic *B*. (B) Non-linear regression analysis of Ca^{2+}_o potency in the absence and presence of *nor*-calcimimetic B with an allosteric ternary complex model (equation 2) where the pK_B is constrained between pathways or not (as indicated).

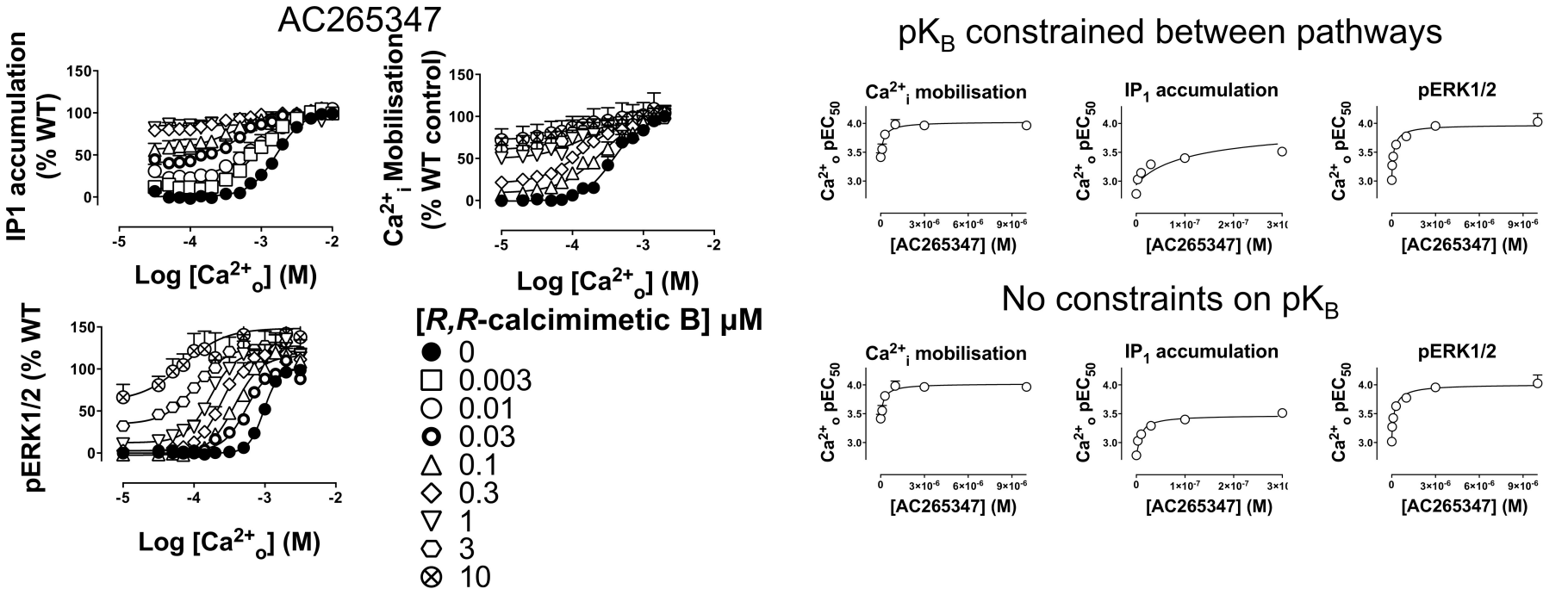

Supplemental Figure 8 AC-265347 potentiation of Ca^{2+}_o-mediated signalling. (A) Ca^{2+}_o stimulation of IP_1 accumulation, Ca^{2+}_i mobilisation and pERK1/2 in the absence and presence of AC-265347. (B) Non-linear regression analysis of Ca^{2+}_o potency in the absence and presence of AC-265347 with an allosteric ternary complex model (equation 2) where the pK_B is constrained between pathways or not (as indicated).

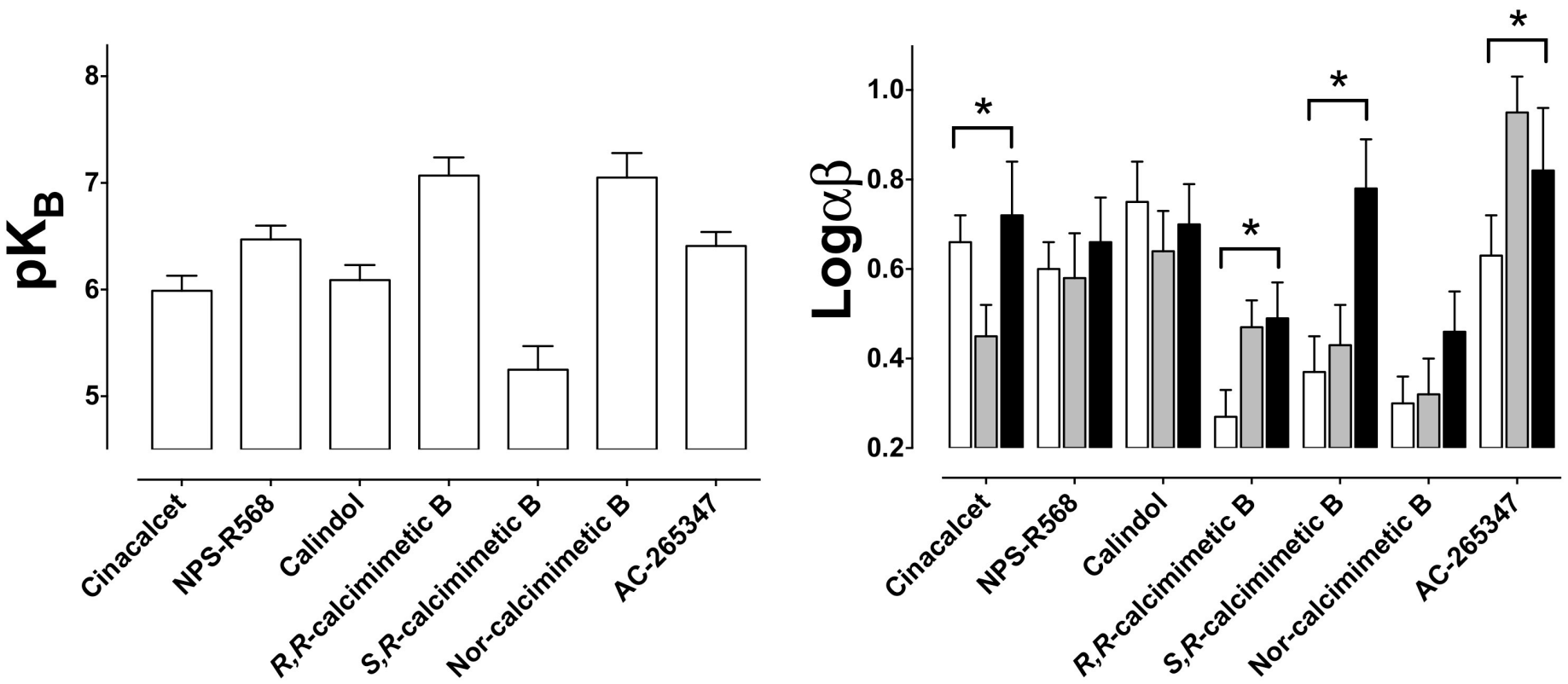

Supplemental Figure 9 Binding affinity and cooperativities of calcimimetics across different pathways. Cooperativities of calcimimetics in Ca^{2+}_i mobilisation (white bars), pERK1/2 (grey bars) and IP_1 accumulation (black bars) assays were determined with the binding affinity constrained to be the same in each assay.

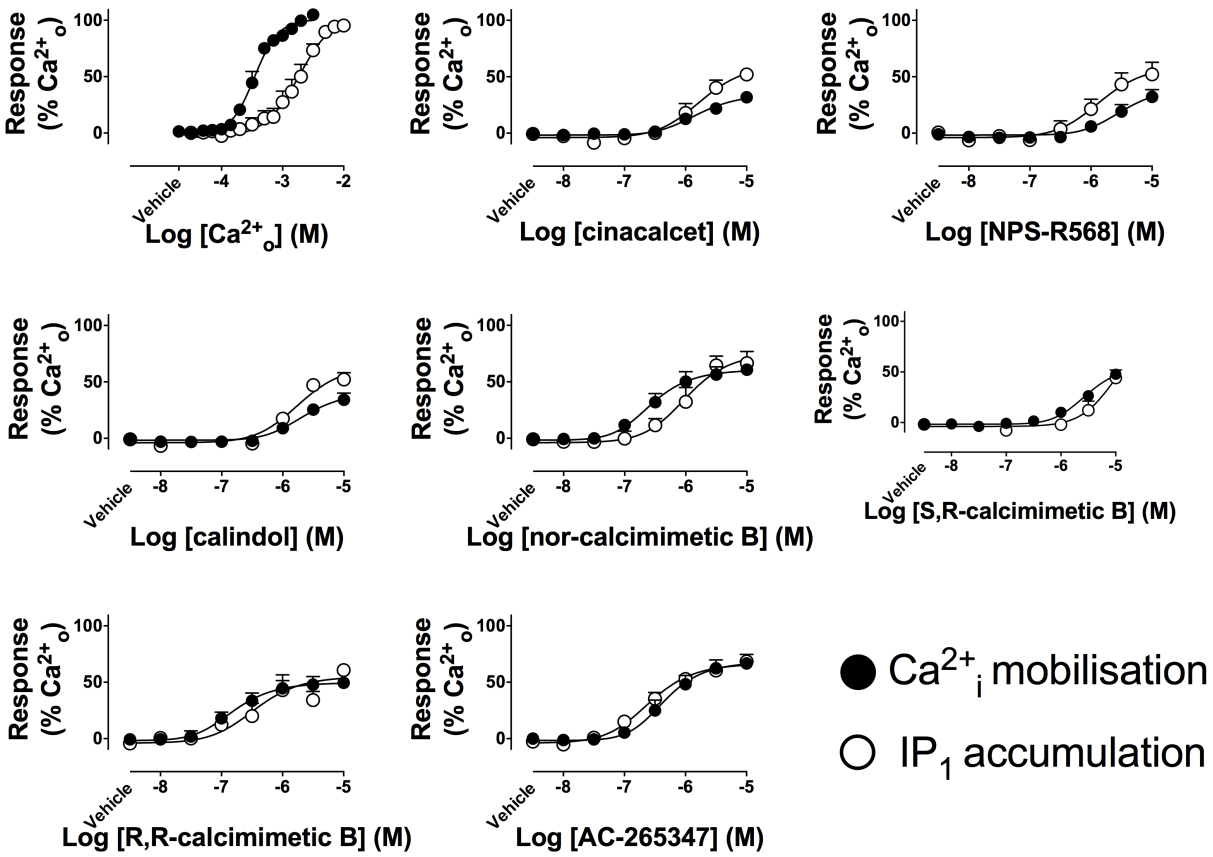

Supplemental Figure 10 Concentration-response curves to Ca^{2+}_o and calcimimetics in the presence of 1.8mM ambient (buffer) Mg^{2+}_o but no Ca^{2+}_o.

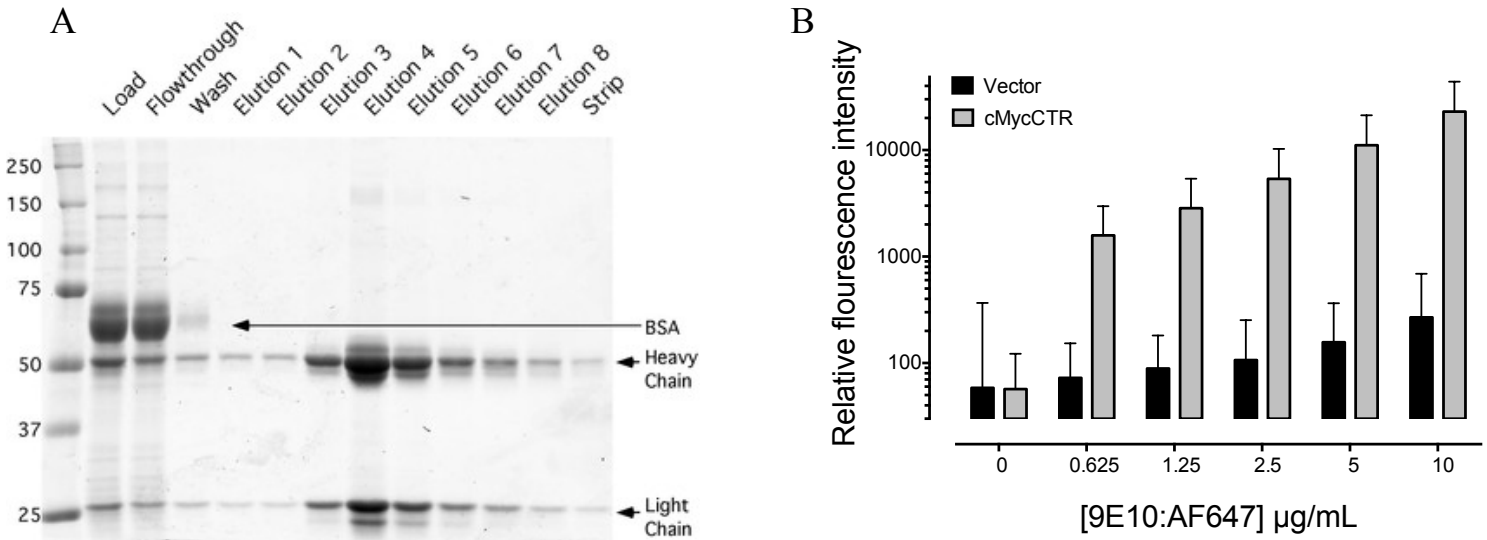

Supplemental Figure 11 Validation of 9E10:AF647 antibody. A) Coomassie stained gel imaged on Typhoon Trio (GE Lifesciences) showing purification of 9E10 antibody from biorector hybridoma supernatant. Molecular weight markers are indicated on the left and various purification fractions indicated above the gel. Densitometry on elution fractions 3-6 was performed using ImageJ and these fractions pooled for the subsequent conjugation reaction. Densitometry was consistent with antibody being >90% pure. Staining is consistent with the concentration as determined by A_{280}. B) Titration of 9E10:AF647 in Cos7 cells stably transfected with either vector control (Vector) or vector containing cMyc tagged calcitonin receptor (cMycCTR). Relative fluorescence intensity corresponds to antibody binding, determined on a FACS CantoII (BD Biosciences), as described in the supplemental methods.

References

Bringmann, G., and Geisler, J.P. (1989). Enantiomerically pure oxygenated 1-phenylethylamines from substituted acetophenones: by reductive amination and regiospecific benzylic cleavage. *Tetrahedron Lett.* ***30*****:** 317–320.

Harrington, P.E., Jean, D.J.S., Jr, Clarine, J., Coulter, T.S., Croghan, M., Davenport, A., et al. (2010). The discovery of an orally efficacious positive allosteric modulator of the calcium sensing receptor containing a dibenzylamine core. *Bioorg. Med. Chem. Lett.* ***20*****:** 5544–5547.

Andreassen KV, Hjuler ST, Furness SG, Sexton PM, Christopoulos A, Nosjean O*, et al.* (2014). Prolonged calcitonin receptor signaling by salmon, but not human calcitonin, reveals ligand bias. *PLoS One* 9**:** e92042.

Leach K, Wen A, Cook AE, Sexton PM, Conigrave AD, Christopoulos A (2013). Impact of Clinically Relevant Mutations on the Pharmacoregulation and Signaling Bias of the Calcium-Sensing Receptor by Positive and Negative Allosteric Modulators. *Endocrinology* 154**:** 1105-1116.